Continental Shelf Research 94 (2015) 28–41

Contents lists available at ScienceDirect

Continental Shelf Research

journal homepage: www.elsevier.com/locate/csr

Research papers

Influence of an upwelling filament on the distribution of labile fraction of dissolved Zn, Cd and Pb off Cape São Vicente, SW Iberia

Carlos Eduardo Monteiro [1], Sara Cardeira, Alexandra Cravo, Maria João Bebianno, Ricardo F. Sánchez [2], Paulo Relvas *

CIMA, FCT, University of the Algarve, Campus of Gambelas, 8005-139 Faro, Portugal

ARTICLE INFO

Article history:
Received 31 March 2014
Received in revised form
9 December 2014
Accepted 18 December 2014
Available online 23 December 2014

Keywords:
Upwelling
Filaments
Dissolved metals
Metal transports
Cape São Vicente
Iberian Peninsula

ABSTRACT

Under northerly winds upwelling is recurrent at the Cape São Vicente, SW Iberia, and plays a major role on the distribution of dissolved nutrients and metals. The aim of this work was to characterize the dissolved metals distribution of zinc (Zn), cadmium (Cd) and lead (Pb), associated with a filament of upwelled water that stretches seaward from the Cape. Additionally, the relationships between labile metals and other oceanographic parameters, such as current velocity and wind field patterns, temperature and salinity, nutrients, chlorophyll *a* and suspended solids were evaluated. The mass transport of the dissolved metals exported offshore was estimated, after a period of relatively strong and persistent upwelling. At the end of October 2004 a total of 42 CTD Rosette casts up to 400 dbar were sampled, distributed on an almost regular grid, together with along-track Acoustic Doppler Current Profile (ADCP) velocities. Seawater samples from two transects across the filament were analysed: one closest to the shore, where upwelling was intense and phytoplankton noticeably grew; and another further offshore where the filament was still well defined, but narrower and less marked despite with the maximum velocity currents. Labile dissolved metals were determined using anodic stripping voltammetry (ASV). The range of the metals recorded at the transect closest to the coast recorded was 0.26–3.8 nM (mean: 0.8 nM) for Zn, 2–11 pM (mean: 3 pM) for Cd and 8–60 pM (mean: 13 pM) while for the offshore transect was: 0.26–5.1 nM (mean: 1.2 nM) for Zn, 2–26 pM (mean 4 pM) for Cd and 8–74 pM (mean: 15 pM). Zinc recorded the highest concentrations, similar at both transects, and like Cd the lowest concentrations were found at near-surface depths. In opposition, the highest Pb concentrations were found at the near-surface depths at the northern stations in both transects. The filament exported more material in the offshore transect than in the transect closest to the coast, corresponding to a maximum export of $\sim$135 kmol d^{-1} of Zn, 276 mol d^{-1} of Cd and $\sim$1365 mol d^{-1} of Pb. The quantification of the cross-shelf fluxes imposed by the filament did show that metals fluxes are strong enough to play a key role in the oceanographic behaviour of the transition zone between the coastal and offshore waters in the region. Considering the periods of strong upwelling events and the extent of their duration along the year, the amounts of exported water mass which include nutrients, metals and particles must be hugely increased and responsible for the high productivity of the waters.

1. Introduction

Portuguese coastal upwelling results from northerly winds due to the northward displacement of the Azores high pressure cell and the weakening of the Iceland low pressure cell during the summer season. The seasonal pattern of the wind direction leads to changes in the Iberian oceanic surface circulation throughout the year (Cotté-Krief et al., 2000). As a consequence of this large scale climatological interplay, an equatorward surface current is established during the summer season as a geostrophic response to the upwelling that occurs along the western Iberian shelf. Continuity implies that subsurface water replaces the surface water, which is driven to the right in relation to the wind and taken offshore due to the Ekman mechanism. Upwelled subsurface water at the coast is cold, causing the decrease in sea surface temperature (SST) and its enrichment in nutrients from deeper levels increase the biological productivity (Cotté-Krief et al., 2000;

* Corresponding author. Current address: CCMAR, University of Algarve, Campus of Gambelas, 8005-139 Faro, Portugal.
E-mail addresses: cessmonteiro@gmail.com (C.E. Monteiro), prelvas@ualg.pt (P. Relvas).
[1] Current address: IPMA, Portuguese Institute of Sea and Atmosphere, Division of Environmental Oceanography and Bioprospection, Av. Brasília, 1449-006 Lisboa, Portugal.
[2] Current address: Centro Oceanográfico de Cádiz, Muelle de Levante s/n, P.O. Box 2609, E-11006 Cádiz, Spain.

http://dx.doi.org/10.1016/j.csr.2014.12.004
0278-4343/

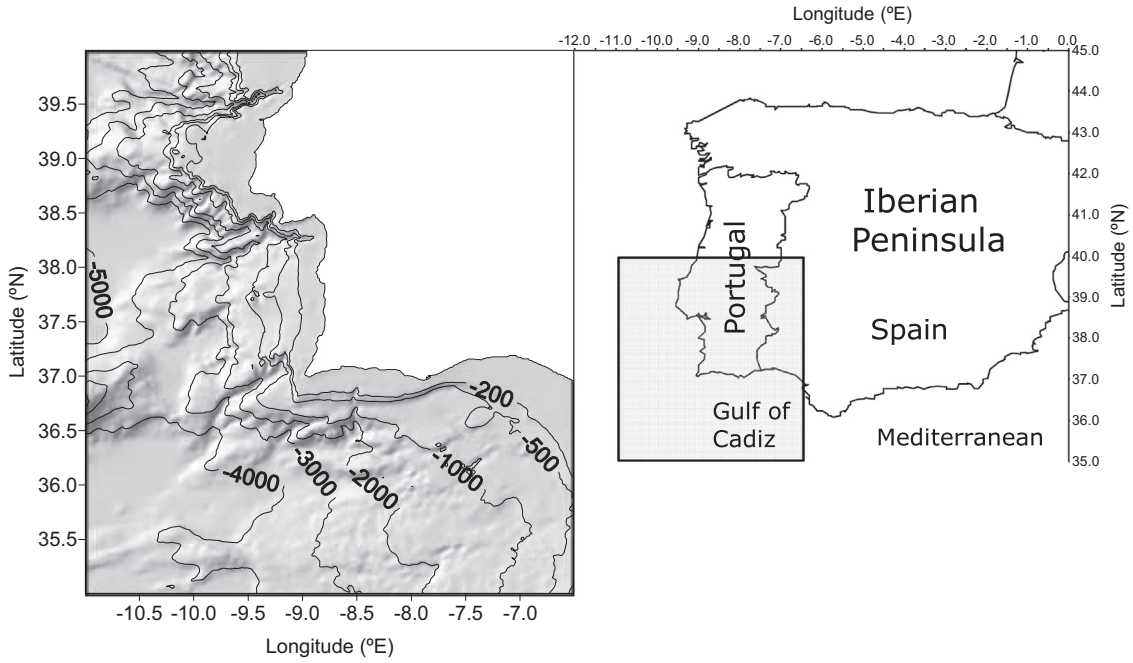

Fig. 1. Location of the study area. Bottom topography and some bathymetric contours are represented, in metres, for the shaded area.

Relvas and Barton, 2005; Relvas et al., 2007; Rossi et al., 2013).

During the upwelling process, a cold filament is recurrently formed off Cape São Vicente, the SW tip of the Iberian Peninsula (Fig. 1). It shows a jet structure stretching westward and exchanging almost one Sverdrup ($1\ Sv = 10^6\ m^3\ s^{-1}$) of water between the coastal and open waters (Sánchez et al., 2008). This means that under upwelling events important offshore mass exchanges are not limited to nutrients but also comprise metals (Cotté-Krief et al., 2000; Biller and Bruland, 2013), among other materials. Consequentially, filaments represent very important structures controlling the ocean productivity (Alvarez-Salgado et al., 2001; García-Muñoz et al., 2004; Cravo et al., 2010; Rossi et al., 2013).

Some trace metals play a key role in biogeochemical processes in the water column, such as zinc (Ellwood and van den Berg, 2000; Franck et al., 2003; Wyatt et al., 2014) and cadmium (Abe, 2005; Cox et al., 2006; Baars et al., 2014), acting as micronutrients (Bruland and Lohan, 2003; Biller and Bruland, 2013; Wyatt et al., 2014), while others like Pb are not required biologically (Bruland and Lohan, 2003). Their vertical patterns of distribution and behaviour associated with upwelling events are not well described in literature (Biller and Bruland, 2013; Valdés et al., 2008).

In the ocean, trace metals generally occur at low concentrations, within the range 10 μM to 1 fM, and particularly for Zn: 0.05–9 nM; Cd: 1–1000 pM and Pb: 5–150 pM (Bruland and Lohan, 2003). The oceanic biogeochemistry of Zn, Cd and Pb, as well as their distribution, can be divided in two main groups: nutrient- and scavenged-type distributions, respectively (Bruland and Lohan, 2003). The first type shows a vertical distribution similar to the nutrients, usually depleted at surface layers contrasting with the increase of concentrations in depth. This distribution is mainly regulated by the plankton consumption in surface waters or euphotic zone (González-Dávila, 1995; Valdés et al., 2008; Pohl et al., 2011), or adsorption onto the particles surface, and followed by oxidation and remineralization from the sinking material in deeper waters, increasing their concentrations, also linked with the biogeochemical cycles of other elements such as the C, N, S and O (Bruland and Lohan, 2003). In addition, these metals can be accumulated at horizontal interfaces/boundaries such as the pycnocline because the velocity of the sinking particles is slow (Pohl et al., 2011). The last type presents an increase at surface layers with a significant decrease in depth due to a highly reactive behaviour, caused by strong interactions with particles (Bruland and Lohan, 2003). These reflect the high affinity to adsorb onto solid surfaces and be removed from solution in the surface layers (Muller, 1999; Brown Jr. and Parks, 2001; Cobelo-García et al., 2005; Santos-Echeandía et al., 2012). The residence time varies depending on the region (coastal or open ocean), distribution profile and is intimately related with the physical, chemical and biological processes in which the metals are involved. Residence times for Zn and Cd are estimated ~50,000 years in the whole ocean (Croot et al., 2011; http://www.mbari.org/chemsensor/pteo.htm in Bruland and Lohan (2003)) and can be used as indirect proxies of past nutrient conditions (Bruland and Lohan, 2003; Croot et al., 2011). Residence time for Pb (~100–1000 yr) induced by its reactive behaviour is lower than for Zn and Cd.

Metal concentrations can be affected by multiple factors rather than the physical forcing including also the inputs either natural or from anthropogenic origin (Saager et al., 1997; Kremling and Streu, 2001; Cotté-Krief et al., 2002; Valdés et al., 2008; Biller and Bruland, 2013). Their major sources are rivers, atmospheric dust, bottom sediments, and hydrothermal vents (Bruland and Lohan, 2003). Phytoplankton has an important role on the cycling and distribution of essential metals. Zinc is an ubiquitous metal and essential to biological activities (Morel and Price, 2003; Bruland and Lohan, 2003; Wyatt et al., 2014). Particularly in some species of diatoms it is involved in the carbonic anhydrase (CA) activity (Morel and Price, 2003) and in one coccolithophore species, it regulates the alkaline phosphatase activity (Shaked et al., 2006). Despite the controversial opinions about Cd behaviour (Morel et al., 1991; European Commission, 2002; Prego et al., 2013), some authors agree about Cd biological functions, which include competition with Zn bioavailability in CA activity under Zn-limited conditions (Morel et al., 1991; Morel and Price, 2003). Both metals have a nutrient-type distribution in the ocean (Bruland and Lohan, 2003; Wyatt et al., 2014), often strongly correlated with the phosphate, nitrate and silicic acid (Bruland and Lohan, 2003; Croot et al., 2011; Wyatt et al., 2014). Conversely, Pb is a non-essential

metal to organisms, with no biological function, which turn it an excellent element to trace anthropogenic inputs to the ocean, since its presence in the ocean is originated by anthropogenic influence. Lead above certain amounts/concentrations may represent an environmental threat by its toxicity (European Commission, 2002; Prego et al., 2013). Zinc, Cd and Pb depicting different behaviours in the ocean were selected for this study to characterise their contribution in an area where upwelling events are recurrent.

Upwelling in the Portuguese coast has been studied for the past years by several researchers from several points of view: (i) physical (Fiúza, 1983; Sánchez et al., 2008); (ii) biological (Moita, 2001; Rossi et al., 2013) and (c) chemical (Cotté-Krief et al., 2000; Cravo et al., 2010). The dynamics and nutrients characterisation of the ocean in SW Iberian region is relatively well known at Cape São Vicente, but our understanding about trace metals and its distribution in the water column associated with upwelling events is poor. To our knowledge this study provides the first attempt to describe data on dissolved metal concentrations in a filament formed during an upwelling event at the SW Iberia, which constitutes an important and innovative approach.

So, the present research aims were to (i) determine the distributions of labile fraction of the dissolved metals in the filament formed during an upwelling event, (ii) relate trace metals distribution with other concurrent oceanographic parameters, such as temperature, salinity, nutrients, chlorophyll *a* (used as a proxy of phytoplankton biomass) and suspended solids, and (iii) estimate the exchange of zinc, cadmium and lead with the offshore waters imposed by the filament. This paper follows other two papers dedicated to this filament, complementing the interdisciplinary study of the Cape São Vicente upwelling filament. Previous papers focused on the physical description of the filament structure (Sánchez et al., 2008) and on the chlorophyll *a* and nutrient export through the filament (Cravo et al., 2010).

2. Material and methods

2.1. Regional hydrography

The Cape São Vicente is located at 37.0°N and 9.0°W, on the southwestern edge of the Iberian Peninsula where the west and south coast meet at almost right angle (Fig. 1). There, the shelf is generally narrow, about 10 km wide in the west coast and 25 km wide in the south coast. The Cape São Vicente region constitutes the southern end of the Iberian segment of the Canary Current Upwelling Systems (CCUS), one of the four Eastern Boundary Upwelling Ecosystems (EBUEs), along with the California, Humboldt and Benguela Currents systems (e.g. Chavez and Messié, 2009; Fréon et al., 2009). Therefore, the region is under the common features that govern these large scale ecosystems: equatorward trade winds forces the offshore Ekman transport in the upper layers over the continental shelf, inducing the upwelling of cold subsurface nutrient-rich waters compared to warmer superficial waters, associated with a broad slow moving equatorward current over the continental shelf and a poleward undercurrent at deeper levels over the continental slope (Smith, 1995; Chavez and Messié, 2009).

The Cape São Vicente represents the discontinuity of the CCUS imposed by the Mediterranean entrance that separates the Iberian Peninsula from the North Africa. Hence, superimposed to the large scale pattern described in the previous paragraph, the specific mesoscale dynamics of the region dominates the ecosystem functioning. We can define three preferred circulation pathways at Cape São Vicente (Relvas and Barton, 2002). The most persistent is the eastward current along the south shore that advects water upwelled off the west coast that turned cyclonically around the Cape São Vicente, merged with the local upwelled water. At relaxation times this flow begins to separate from the coast due to a warmer countercurrent originated in the Gulf of Cadiz that progress westward attached to the coast. The second pattern results from the development of a cold water filament rooted in the Cape São Vicente, which progress to the south sustained by the upwelling further north and extends more than 150 km far from the cape at times. The third is the development of the upwelling filament to the west of the cape, eventually due to the instability of the equatorward upwelling jet (Sánchez et al., 2008; Relvas and Barton, 2002). Nevertheless, this filament, physically described by Sánchez et al. (2008), is of major importance regarding the transfer of matter between coastal and open waters. Due to the narrow shelf and complex topography, intense eddy activity is observed giving origin to a large potential for cross-shelf export, as it occurs in most regions of the CCUS (Arístegui et al., 2009; Rossi et al., 2013).

2.2. Sampling and methods

Data used in this paper were collected on board of the Portuguese navy R/V "D. Carlos I" during a survey carried out during 22–25 October of 2004, as described in Cravo et al. (2010). Sampling took place in 42 casts using a Rosette sampler coupled with 12 PVC bottles (*Niskin General Oceanics*, Model 1010, stainless steel spring with Teflon, and latex tubing, acid cleaned previously to the cruise) to collect water samples at 10 depths: 5 (surface), 10, 20, 30, 50, 75, 100, 150, 200 and 400 dbar. CTD data were gathered by a CTD *Idronaut* OS 316 coupled to the Rosette system, lowering at 1 ms^{-1} with a sampling rate of 20 Hz by a steel wire on the winch.

The sampling strategy was guided by near real-time satellite imagery data, as shown in Fig. 2, when a clear signature in the sea surface temperature was observed prior to the cruise. In this paper data are presented only for two transects, one identified as transect II, closest to the shore where upwelling was intense and phytoplankton markedly developed (Cravo et al., 2010), and the other identified as transect IV, 40 km further offshore where the filament jet was narrower but still well defined (Sánchez et al., 2008).

Water samples for dissolved labile metals determination were collected in low-density polyethylene (LDPE) bottles previously decontaminated with 10% Aristar HCl Ultra, BDH (filled with diluted 10% HCl Aristar Ultra, BDH until the moment of water collection) and then immediately filtered through Pall Gelman filters GN-6 (mixed cellulose esters), of 0.45 μm porosity. The filters were also previously decontaminated with diluted Aristar HCl Ultra, BDH and rinsed with deionised water (Milli-Q). On shipboard, samples were not processed under filtered air. After filtration, samples were acidified with HCl 30% to pH < 2 to keep the metals in solution and preserved for later analysis, kept in closed plastic zipped bags inside PVC boxes. All the glassware filtration apparatus was also washed with 10% Aristar HCl Ultra, BDH, left in a bath during a week and afterwards washed in ultrapure water and finally with deionized water, quality Milli-Q.

Analysis were carried out by standard addition method using anodic stripping voltammetry (ASV) performed in a 746 VA Trace Analyser (Metrohm) coupled with 747 VA Stand (Metrohm), using a borosilicate glass voltammetry cell. A hanging mercury dropping electrode (HMDE) was used, a Ag/AgCl (KCl) was used as the reference electrode while a carbon rod was used as the counter electrode. All samples were purged at least 15 minutes with gaseous N_2 at 1.2 bar for oxygen removal from the solution. The deposition step was set to 300 s. For the stripping step a linear sweep between -1150 mV and 300 mV was applied. The peaks were recorded for each of the studied metals and the concentration calculated as proportional to the height of the peak (as described

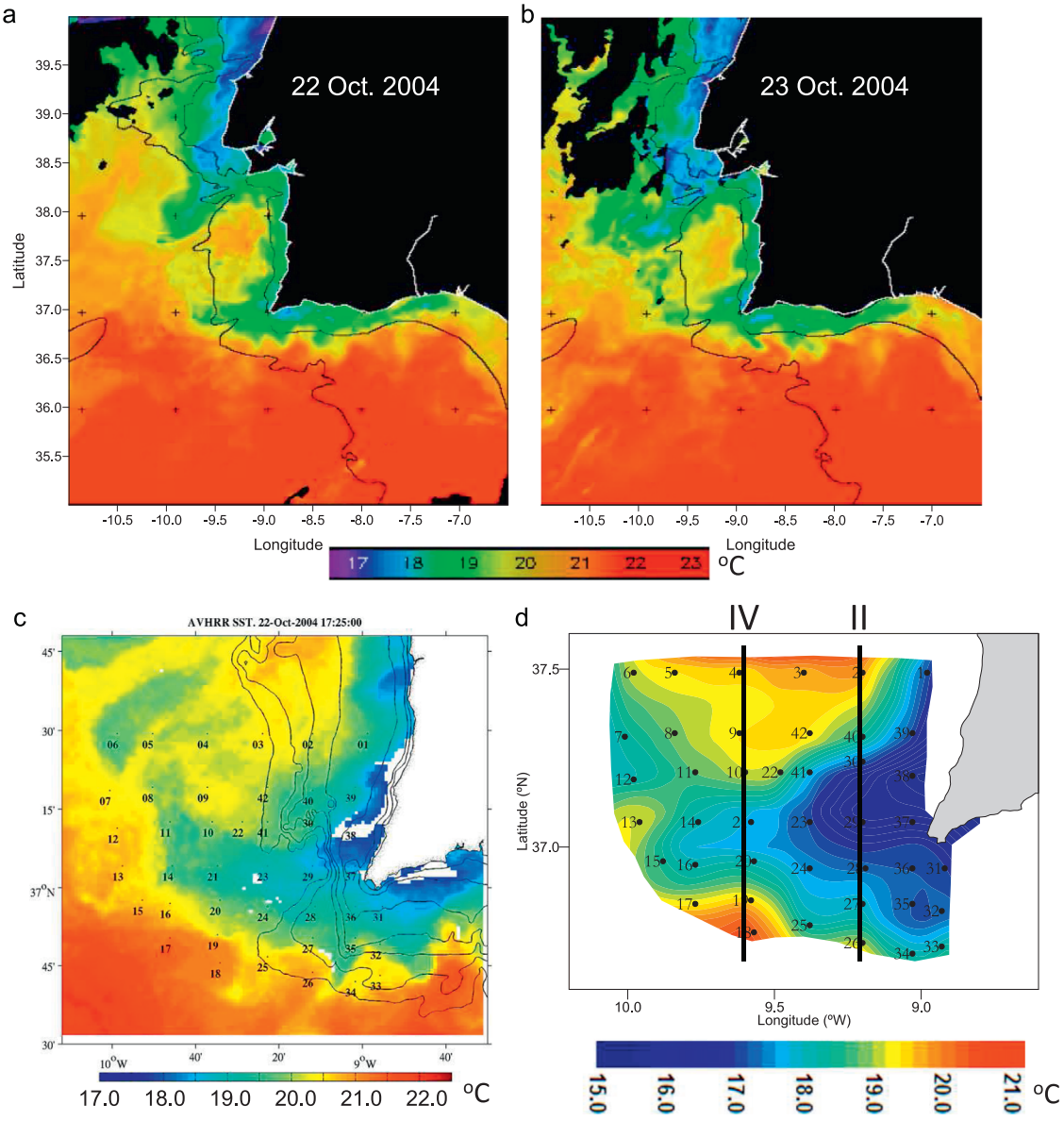

Fig. 2. Signal of the upwelling filament on the Sea Surface Temperature (SST) field. (a and b respectively) AVHRR NOAA series satellite images from 22 and 23 October 2004. (c) SST image from 22 October 2004 with the filament region enlarged and the sampled CTD stations superimposed. (d) Temperature field at 30 dbar constructed through objective analysis upon the direct observations. CTD stations and the two analysed transects are represented, identified as transect II and transect IV.

by the Metrohm producer; Abe et al., 1983). During the metals analysis, the polarography equipment was maintained within a laminar flow hood. Analytical accuracy was constantly checked using the seawater certified reference material NASS-4 (National Research Council of Canada, 1992). All results ($n=7$) were in good agreement with the certified values: Zn 2.95 ± 0.25 nM (certified 2.72 ± 0.38 nM), Cd 136 ± 24 pM (certified 142 ± 27 pM) and Pb 59.4 ± 22 pM (certified 62.7 ± 24.1 pM). Recovery ranged from 95% (Pb) to 107% (Zn). All analysis procedure was controlled by analysing blanks and using standard addition method, repeated in every 20 samples to insure that there was no cross contamination and the equipment was operating at the same conditions. Replicate of samples were also used to assess variability of the data. Zinc concentrations did show a few anomalous values. Those were carefully examined by comparing with historical data and some of them were rejected as outliers.

Detection limits (calculated from 3 times the standard deviation of the blank analysis) were 0.26 nM for dissolved Zn, 2 pM for dissolved Cd and 8 pM for dissolved Pb. Precision was calculated as $\pm 7\%$ for Pb and as $\pm 4\%$ for Cd and Zn. Detailed procedures for the analyses of concurrent samples for dissolved oxygen, nutrients, chlorophyll *a* and suspended solids determinations are described in Cravo et al. (2010).

Current velocities were measured along the ship track using a hull-mounted 38 kHz RDI acoustic Doppler current profiler (ADCP). Details about the data processing, including the removal of the tidal currents from the velocity data, and the observed velocity field can be found in Sánchez et al. (2008). Due to the ADCP configuration, velocities in the top 30 m of the water column were not directly sampled. Since some parameters revealed relatively high values in the surface layer, geostrophic velocities computed from the dynamic height of the sea surface relatively to the 400 dbar reference depth were used in the top 30 m. Velocities perpendicular to the filament cross transects were objectively interpolated onto a regular grid. The dissolved metal concentrations were interpolated onto the same grid. The horizontal advective fluxes were computed at each grid node by multiplying the velocity by the correspondent variable value. Transports were

calculated by spatially integrating the fluxes over the desired region.

3. Results

3.1. Wind

Fig. 3 displays the mean satellite QuikSCAT winds for a 1° × 1° box around Cape São Vicente in September–October 2004. The October 2004 low-passed winds recorded every three hours at the Sagres meteorological station, located on the Cape São Vicente cliffs and well exposed to the coastal winds, are also shown. QuikSCAT winds reveal that northerlies were strong and persistent from September through October 2004, with two major periods of relaxation: one between 8–10 October and another between 17–27 October. The independent sampling carried out on land confirms and details this wind pattern.

The cruise period (22–25 October, shaded grey area in Fig. 3) occurred during this second relaxation period, after a long period of northerly winds, favourable to upwelling off the western coast. A few days before the cruise, the wind direction changed, blowing predominantly from south and southwest, revealing the decaying stage of the upwelling season (April–October). Towards the end of the cruise northerlies intensified again. However, previous northerlies induced the filament formation offshore Cape São Vicente and its westward stretching was preserved until late October, perhaps in a decaying phase. If we consider the peak upwelling favourable wind velocity prior to the cruise (7.5 ms^{-1}, 11–16 October) to compute the Ekman transport in the most offshore transect (located at 9.5°W with 80 km length-transect IV, Fig. 2), it gives about 0.07 Sv (Sánchez et al., 2008), which is strong enough to maintain the filament during our sampling period.

3.2. Thermohaline signature of the filament

The relatively developed upwelling filament was clearly observed in the satellite imagery obtained during the cruise time (Fig. 2), regardless the decrease of the upwelling intensity as a consequence of the weakening of the wind during the campaign. The SST signature of the filament was evident with water temperatures < 18.5 °C, contrasting with the temperature of the surrounding waters > 20.5 °C (Fig. 2). The filament had approximately 80 km of extension (W–E) and an area of about 100 km × 80 km. A cross shore transect of temperature and salinity is shown in Fig. 4, revealing the uplift of the isolines against the coast above 150 m depth, a clear signal that upwelling was still present at the time of the cruise. Accordingly, the isolines of nutrients, dissolved oxygen and density shown in Cravo et al. (2010) follow this pattern (see their Fig. 5).

The isolines elevation at central stations in both transects (Fig. 5), with the shallowing of colder and less saline water from deeper levels, reveal divergence along the filament axis. The signal of the filament structure was seen down to a depth of 200 m, stronger at the more coastal transect (transect II). In transect IV, a trough in the temperature and salinity fields is observed under the filament axis, below ~100 m depth, suggesting convergence at that depths induced by transient features (Sánchez et al., 2008). At deeper levels, below ~350 m depth, a fingerprint of the Mediterranean Water (MW) was identified in the southern flank of these two transects, around 36.9–37°N (Sánchez et al., 2008 – not shown here).

3.3. Flow field

Fig. 6 shows the vertical fields of the zonal *u*-component of the flow velocity, perpendicular to both transects II and IV, observed during the surveyed period. Negative flows are seaward (westward). Both transects are dominated by westward flows, particularly transect IV, the most distant from the coast. The strongest velocities, above 0.3 ms^{-1}, are observed in the shallower layers and shall define the filament jet. The filament core seems broader and deeper in transect IV, interleaved by weak (< 0.1 ms^{-1}) and patchy eastward flows. In transect II the strongest velocities are limited to the near-surface layer and a significant onshore return flow is observed below the main offshore jet. The filament is bounded by a weaker return flow on its southern side. Detailed description of the current pattern fields at the Cape São Vicente can be found in Sánchez et al. (2008).

3.4. Labile fraction of the dissolved trace metal concentrations

The vertical fields of the labile fraction of the dissolved trace metals in transects II and IV are represented in Fig. 7. Zinc concentrations in transect II (0.26–3.8 nM; Fig. 7a) were slightly lower than those in transect IV (0.26–5.1 nM; Fig. 7d). In transect II the area of maximal concentrations encompassed one nucleus around 100–200 dbar, at the central stations of the transect. This illustrates the metal supply as waters uplift during upwelling (Figs. 4 and 5). Below this depth, concentrations increased down to

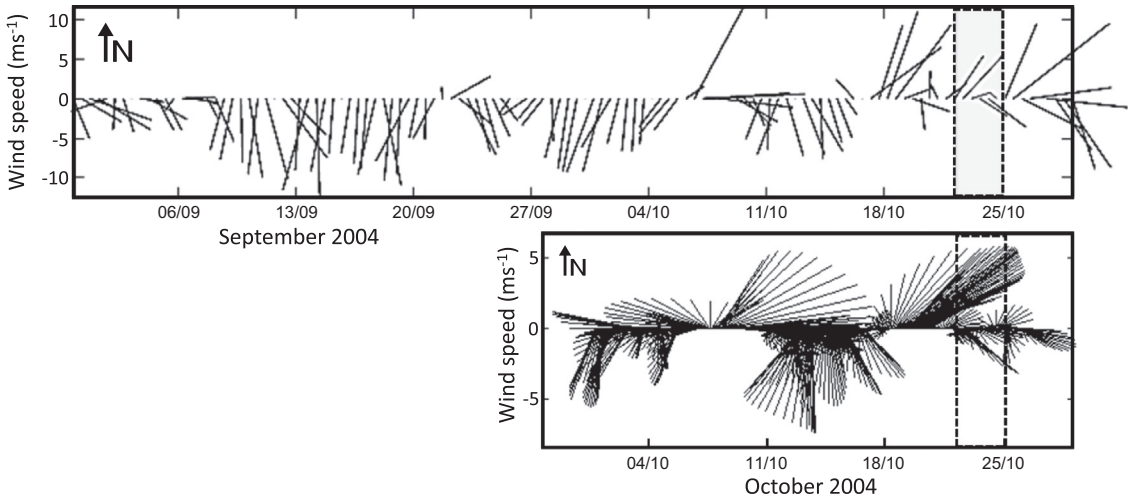

Fig. 3. *Top*: satellite QuikSCAT winds for a 1° × 1° box around Cape São Vicente in September–October 2004. *Bottom*: stick diagram of the low-passed wind velocity recorded at the Sagres meteorological station, from 30 September to 27 October 2004. Dashed lines delimit the cruise period.

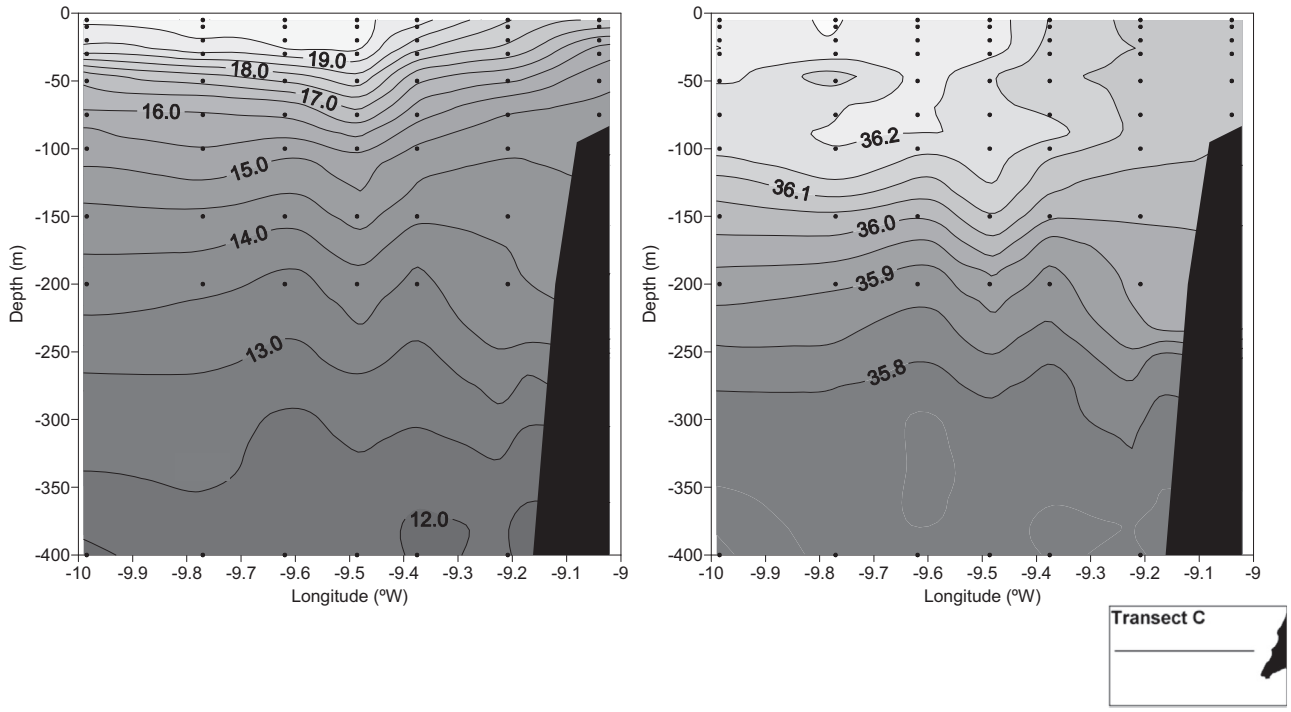

Fig. 4. Vertical fields of temperature (*left*) and salinity (*right*) along a cross-shore transect anchored in the filament root. The rise of the isotherms and isohalines clearly evidence the upwelling pattern.

350 dbar. In transect IV, a core of the highest concentrations from surface down to 50 dbar, by the edges of this section, where the chlorophyll *a* concentrations were lower than in the central stations (see Cravo et al. (2010, Fig. 6)).

Dissolved Cd concentrations had the lowest values from the three dissolved trace metals studied. At both transects II and IV (Fig. 7b and e, respectively) the highest concentrations were above 150 dbar, maximum (28 pM) at Section 4. However, its distribution along the water column varied between transects. In transect II (Fig. 7b), dissolved Cd was not detected (<2 pM) at the near-surface depths, and was maximum (11 pM) between 100 and 150 dbar, across most of the transect. In transect IV (Fig. 7e), where the filament was still well defined, its distribution was circumscribed to the upper layers down to 75 dbar, along the entire transect, maximum at both the north and south edges.

Dissolved Pb concentrations in transects II and IV (Fig. 7c and f, respectively) were particularly low at the central area, where the filament was developed. Lead was highest mainly at the northern stations, from the upper layers down to 200 dbar. This area corresponds to that where the current was dominantly coastward, in opposition to the seaward direction of the filament tongue (Fig. 6). The range of concentrations varied between the detection limit (8 pM) and a maximum 74 pM in transect IV (between 50 and 100 dbar).

In order to determine if there is any oceanographic consistency based on the velocity of the current influence upon the metal distributions, a relationship between the cross-shore ADCP velocity and each element was conducted for both transects and presented in Fig. 8. The analysis show that for both transects the highest concentrations of the three metals occur with the weakest speeds, as seen at the frontal boundary between seaward and shoreward flows (Fig. 6).

3.5. Filament contribution to metal fluxes and transports across the shelf

To determine the contribution of the filament to the metals offshore transport, the horizontal fluxes at both transects were computed (Fig. 9). Table 1 presents an estimate of the metals transported seaward within the filament, from surface down to 200 dbar, in comparison with those transported coastward at both transects. The considered areas comprise the overall extension of both transects ~83.5–84.5 km along the top 200 m (where the uplift of waters was evident).

It should be noted that these values represent rough estimates associated with some kind of uncertainties. Even though, we consider these data valuable, innovative for this region, contributing to the better understanding of the metal loads exchanged through an upwelling filament off SW Iberia. Moreover, the data show consistency with the observed oceanographic features. For the three metals, the seaward flux was noticeably high in the area defined by the filament, particularly in the transect IV, where the velocity of the jet increased (Fig. 6). The estimated offshore transport of metals across the filament is higher in transect IV than in transect II (Table 1). In this last section, fluxes were more intense in an area from the surface until the 75 dbar and in a deeper core from 100 to 200 dbar, around 37.3–37.4°N (Fig. 9d–f). In the surrounding area of the filament, there was onshore return flow, associated to an eddy structure promoting a considerable coastward transport of metals, more evident in transect II (Fig. 9a–c).

The Zn pattern of seaward export in transect II (Fig. 9a) was intensified in a major core, centred at 37.1°N at 50 dbar. If we consider the main centre limited by the -0.1 μmol m^{-2} s^{-1} flux isoline the offshore transport of Zn by the filament is 295 mmol s^{-1} (25 kmol d^{-1}), lower than that estimated in the three main centres for transect IV, that is 1560 mmol s^{-1} (~135 kmol d^{-1}). Zn transported by the filament relatively to the total exported seaward in this section corresponds to 73%, a higher contribution than any of the other metals in both sections (Table 1). In addition, below 200 dbar, the influence of the Mediterranean Water was recorded, as for the other two metals, intensified in the central stations (Fig. 9d–f). For Cd, considering the filament limited by a minimum flux isoline of -0.2 nmol m^{-2} s^{-1}, centred at 37.25°N at 50 dbar and at 37.30°N from 100 down to 200 dbar, the offshore transport in transect IV is 3 mmol s^{-1}

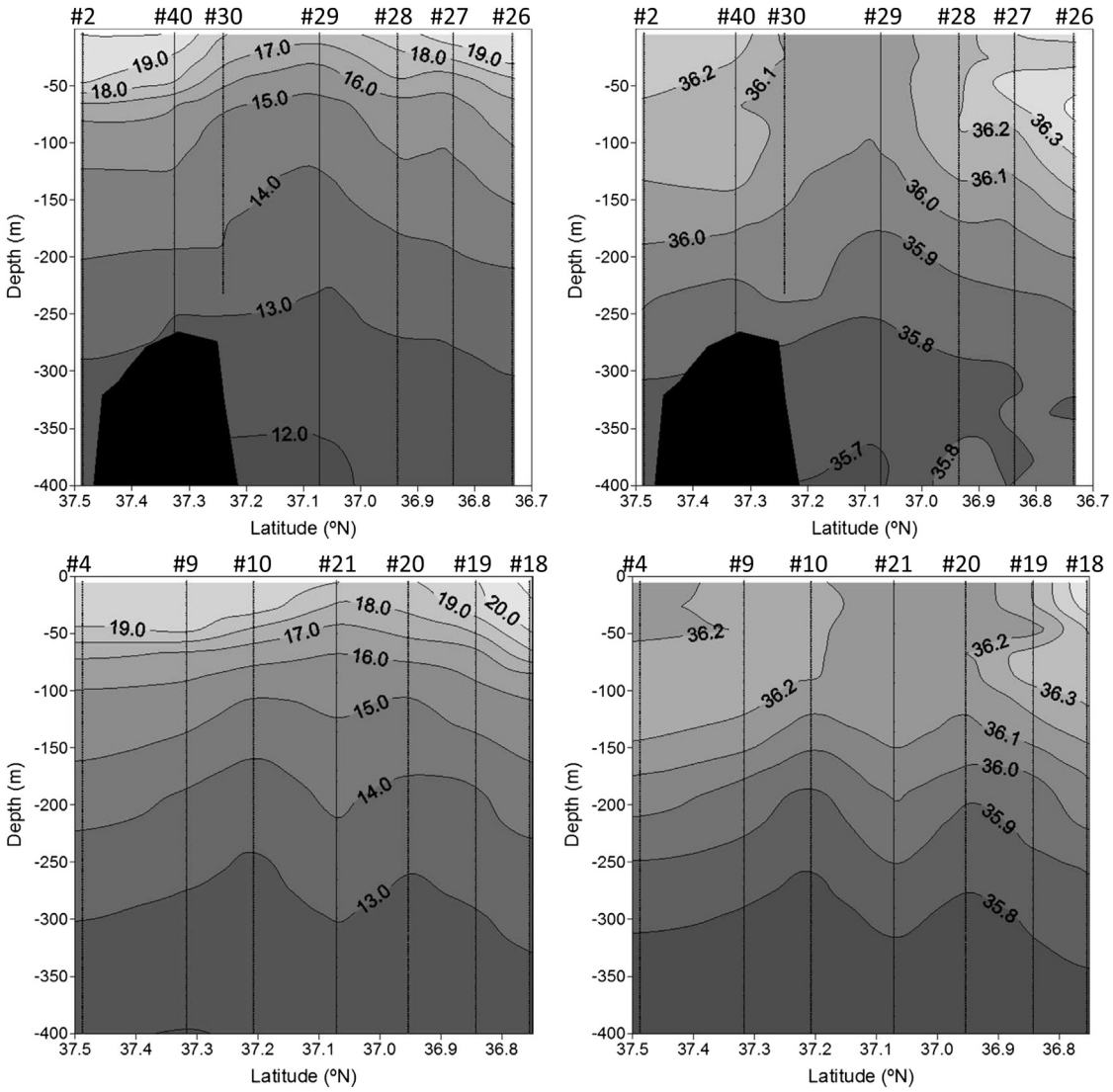

Fig. 5. Signal of the filament in the temperature and salinity vertical fields observed in transect II (a and b respectively) and transect IV (c and d respectively). Stations numbers are displayed in the top axis and dotted lines represent the temperature and salinity readings.

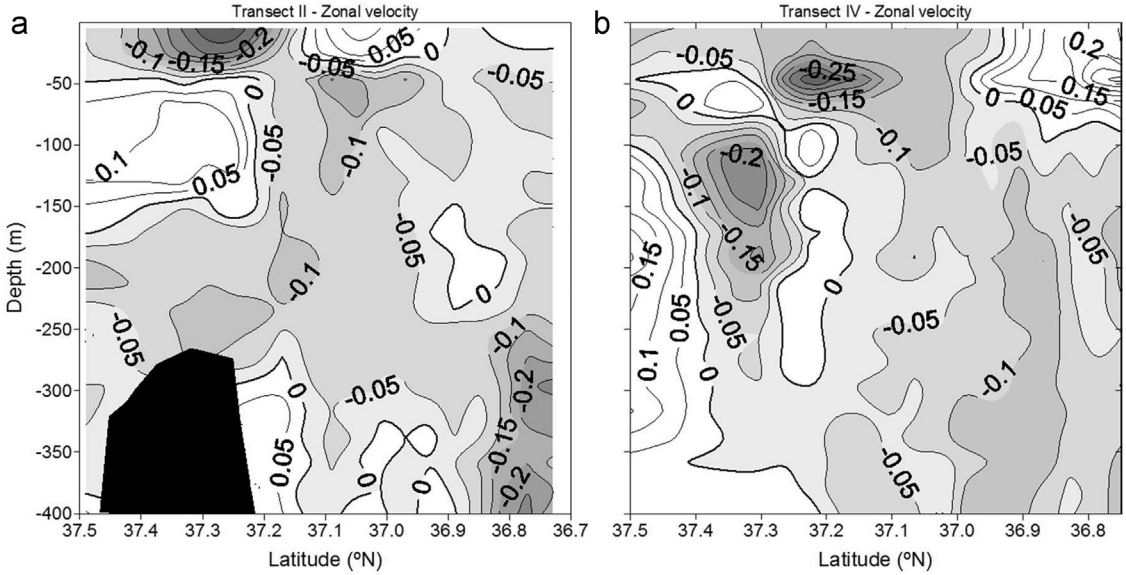

Fig. 6. Vertical fields of the zonal flow perpendicular to transect II (a) and to transect IV (b), in 10^{-2} ms^{-1}. Negative velocities are seaward.

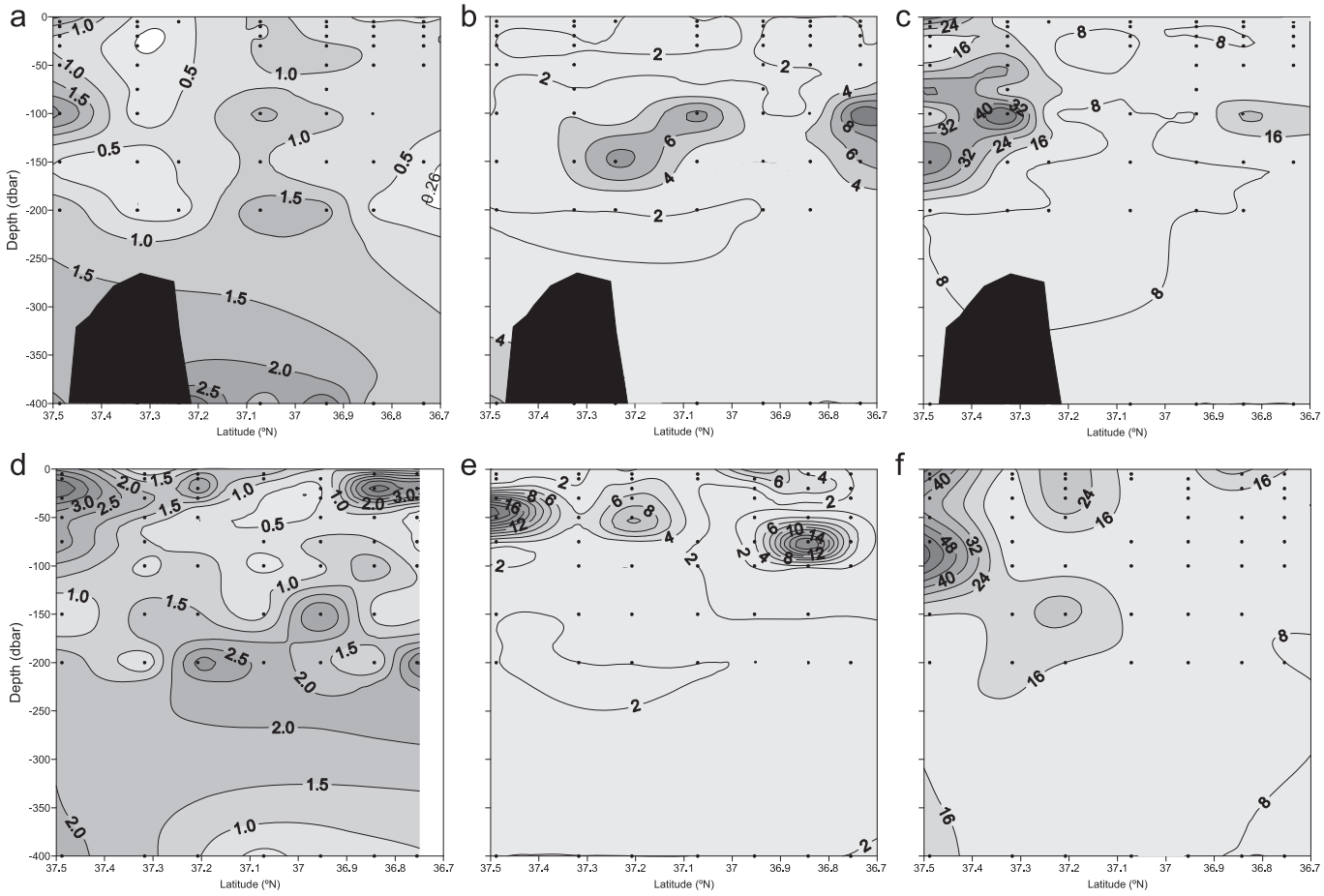

Fig. 7. Vertical fields of dissolved trace metals. Transect II: zinc (a), cadmium (b) and lead (c). Transect IV: zinc (d), cadmium (e) and lead (f). Units: nM for Zn; pM for Cd and Pb. Dots represent the sampling points.

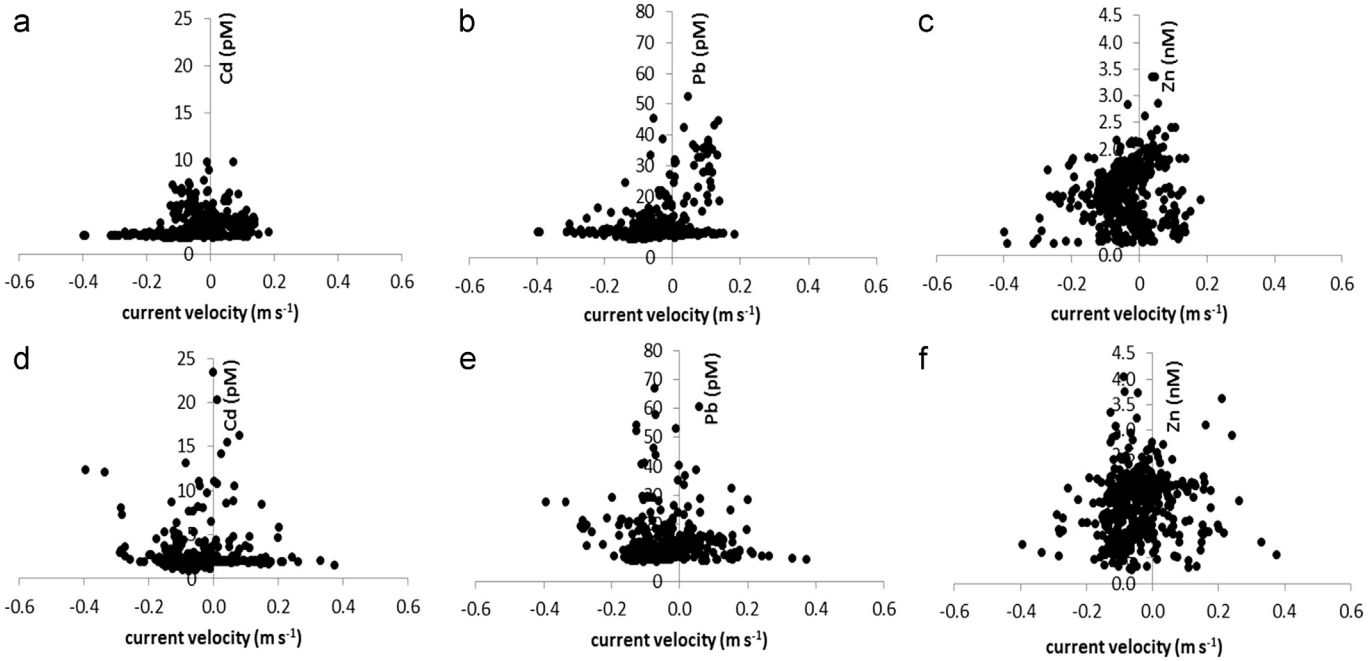

Fig. 8. Relationship between ADCP values (ms^{-1}) and the concentration of each element for both transects: (a) Cd, (b) Pb and (c) Zn for transect II and (d) Cd, (e) Pb and (f) Zn for transect IV.

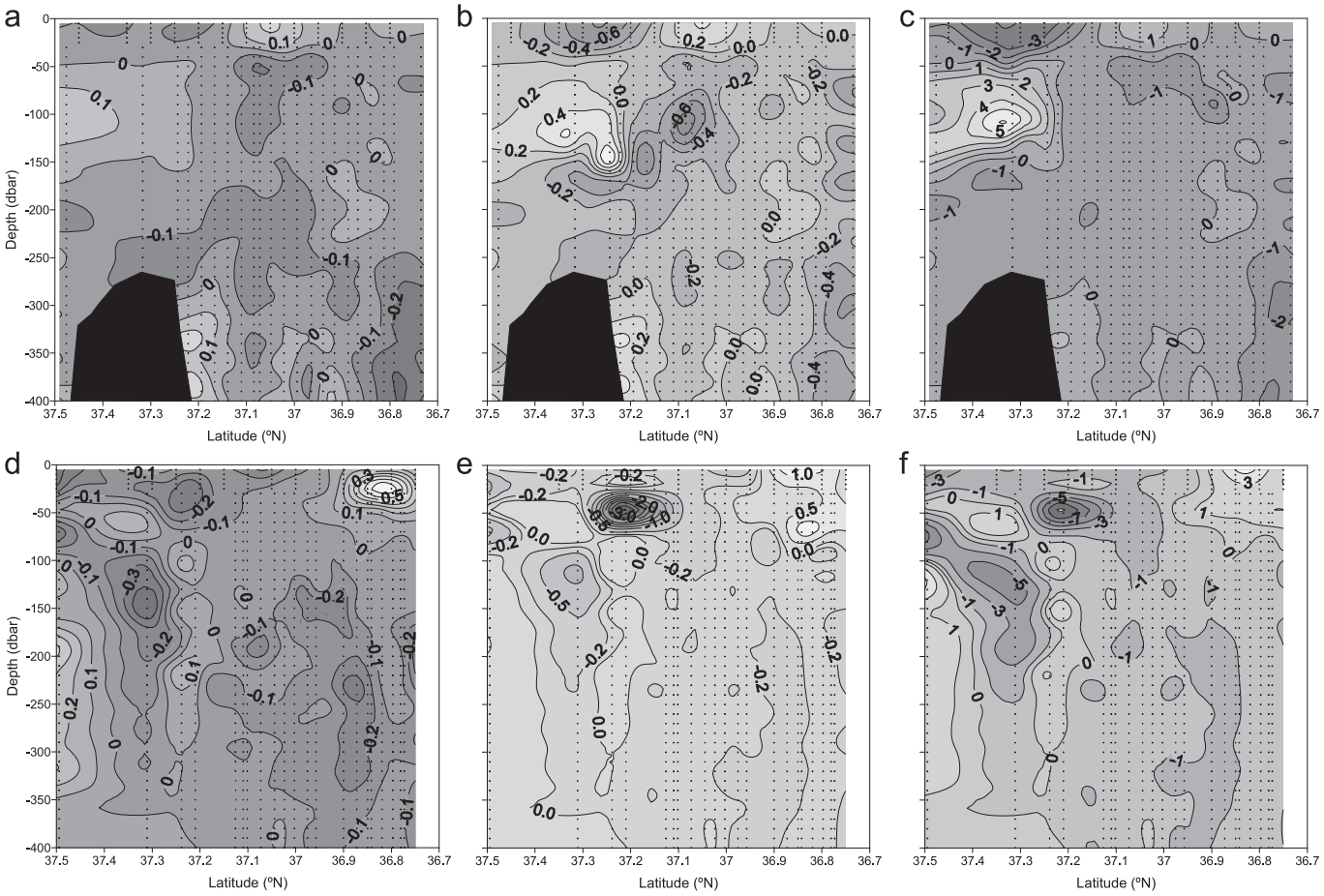

Fig. 9. Fluxes of the dissolved trace metals. Across transect II: zinc (a), cadmium (b) and lead (c). Across transect IV: zinc (d), cadmium (e) and lead (f). Units: μmol m^{-2} s^{-1} for Zn; nmol m^{-2} s^{-1} for Cd and Pb. Negative values mean seaward fluxes. Dots represent the ADCP bins used to define the fluxes.

Table 1
Seaward and coastward mass transport of Zn, Cd and Pb in mmol s^{-1} from surface down to 200 m in transects II and IV. The mass transported seaward through the filament is presented too. The relations between the seaward and the total transports (seaward+coastward) are shown, as well as the relation between the mass transported by the filament and the total exported seaward in the entire section till 200 m depth. The area considered for transects II and IV was 16,890,000 m^2 (84.45 km × 200 m) and 16,668,000 m^2 (83.34 km × 200 m), respectively.

	Seaward	Coastward	%Seaward/Total	Filament	%Filament/Seaward
Transect II Transport (mmol s^{-1})					
Zn	1024	950	52	295	29
Cd	4	3	57	2	50
Pb	15	26	37	5	33
Transect IV Transport (mmol s^{-1})					
Zn	2125	2295	48	1560	73
Cd	6	6	50	3	50
Pb	28	23	55	16	57

(~0.3 kmol d^{-1}), higher than in transect II ~2 mmol s^{-1} (0.1 kmol d^{-1}). However, the contribution of the filament in relation to the total exported seaward for both sections is 50% (Table 1). For this metal, offshore transport in transect IV was similar to that estimated coastward (50%), while in transect II this proportion increase to 57% (Table 1). For Pb, if we consider the filament limited by a minimum isoline of −1.0 nmol m^{-2} s^{-1}, centred at 37.20°N at 50 dbar and at 37.50–37.25 °N from 50 down to 200 dbar it corresponds at section IV to 16 mmol s^{-1} (1.4 kmol d^{-1}) against 5 mmol s^{-1} (0.4 kmol d^{-1}) in transect II. At this last area, the coastward transport of Pb was higher than that estimated seaward. The offshore transport by the filament in transect II represents only 33% of the total while in transect IV it accounts for 57% (Table 1).

4. Discussion

4.1. Labile fraction of dissolved metals fate during upwelling

One of the main goals of this study was to understand how metals behave on the Iberian shelf during upwelling events. The cruise provided a unique opportunity to assess these conditions, complemented by the physical, chemical and biological data (Sánchez et al., 2008; Cravo et al., 2010). Upwelling indeed occurred in the surveyed area, followed by a wind relaxation period (Figs. 2 and 3). Despite the fact that the filament was not in its fully developed stage, there was a clear fingerprint on the dissolved metal distribution, like that observed for nutrients and chl *a* (Cravo et al., 2010).

The number of studies reported in the literature regarding metals concentrations in the Iberian Peninsula coast are limited (e.g. Van Geen et al., 1991; Leal et al., 1997; Cotté-Krief et al., 2000; Caetano and Vale, 2003; Canovas et al., 2007; Santos-Echeandía et al., 2012; Prego et al., 2013; Table 2, this paper). Most of these studies were not particularly devoted to the effect of upwelling upon the distribution of the metals. Like in other coasts, metal concentrations along the Portuguese coast tend to be lower offshore than at the coast, particularly where estuaries outflow (Cotté-Krief et al., 2000; Santos-Echeandía et al., 2012; Prego et al., 2013). At Cape São Vicente there is no significant river runoff

Table 2
Comparison of Zn, Cd and Pb dissolved concentrations, observed in some marine and coastal sites, considering different metal contributions due to regional influence.

Location	Level	Condition	Zn (nM)	Cd (pM)	Pb (pM)	Reference
South Portuguese Shelf (CSV) Transect II	**Surface/water column**	Upwelling	**0.26–3.8**	**2–11**	**8–60**	**Present work**
South Portuguese Shelf (CSV) Transect IV	**Surface/water column**	Upwelling	**0.26–5.1**	**2–28**	**8–74**	**Present work**
Portuguese coast upwelling	Surface		0.9–4.3	30–80		Cotté-Krief et al. (2000)
Portuguese Shelf (close CSV)	Surface		3–20	40–250		Cotté-Krief et al. (2000)
Portuguese Shelf (close CSV)	Surface			61–100		Caetano and Vale (2003)
Portuguese coast (close CSV)	Surface		10–15	150–890	Up to 60	Santos-Echeandía et al. (2012)
Portuguese coast	Surface		1.4–62	10–890	10–150	Santos-Echeandía et al. (2012)
North Iberian Peninsula Shelf (Galicia)	Surface/water column	Upwelling	1.8–13.0	16–156	80–510	Prego et al. (2013)
North Iberian Peninsula Shelf (Galicia)	Surface/water column		4.6–19.1	19–104		Santos-Echeandía et al. (2009)
North Pacific, California Current system	Surface/water column	Upwelling	0.07–6.5	18–1024		Biller and Bruland (2013)
Cape Blanco, Oregon coast, NE Pacific	Surface/water column	Upwelling		~200–900		Takesue and van Geen (2002)
Mejillones Bay, Chile	Surface	Upwelling		89–979		Valdés et al. (2008)
Northeast Atlantic Ocean	Surface/water column		0.1–3.0	20–190	30–220	Cotté-Krief et al. (2002); Ellwood and van den Berg (2000); Kremling and Streu (2001); Saager et al. (1997)
North Atlantic – Gulf of Cadiz	surface - 400 m			< 10–300	< 300	Morley et al. (1997)
SE Spanish coast, Gulf of Cadiz	Surface		10–30	150–190		Elbaz-Poulichet et al. (2001b); Van Geen et al. (1991)
Douro River, Portugal	Surface			$< 2.20 \times 10^3$		Caetano and Vale (2003)
Tagus River, Portugal	Surface			$< 1.50 \times 10^3$		Caetano and Vale (2003)
Douro River, adjoining coast, Portugal	Surface			$9.79 \times 10^3 - 1.42 \times 10^4$	$8.20 \times 10^3 - 1.83 \times 10^4$	Leal et al. (1997)
Tinto and Odiel Rivers, Spain	Surface		$3.37 \times 10^4 - 2.33 \times 10^6$	$9.79 \times 10^4 - 6.05 \times 10^6$	$3.38 \times 10^4 - 3.37 \times 10^6$	Canovas et al. (2007)

contribution, so it is assumed that the recorded metal concentrations are mainly derived by upwelling, where metal concentrations are higher than in nonupwelling open-ocean areas. For Cd, Boyle et al. (1981) had reported for these two distinct areas values in the range 30–50 pmol/kg, higher than <10 pmol/kg, respectively, like in this study. Our data do not support the concept of Cotté-Krief et al. (2000) inferring that upwelling is not important for the enrichment of metals in the coastal zone, rather causing a large dilution of the continental inputs over the shelf. The authors stated that the Portuguese upwelling differs from the more classical systems, what we do not believe in the context of the present results. The low Cd and Pb concentrations may result from the fact that other recurrent upwelling centres could be more productive and consequentially the waters brought from deeper levels are enriched in metals. Even though, their estimates represent important amounts (Table 1), particularly for Zn, in the transect IV (135 kmol d^{-1}). There the filament funnels and the velocity was maximum, which was accompanied by a decrease in the chl *a* concentration relatively to the transect II (Cravo et al., 2010, Fig. 6) that could contribute to a lower consumption of this essential metal.

Table 2 shows that the order of magnitude of the concentrations found in the present research is within that recorded at sites along the south Portuguese shelf waters, close to the Cape São Vicente. For dissolved Zn, values were lower than those reported (0.9–20 nM, Cotté-Krief et al., 2000; 10–15 nM, Santos-Echeandía et al., 2012) for zones near the study area, but closer to the coast. The Cd concentrations were lower than the range reported for this area (150–890 pM), by Santos-Echeandía et al. (2012), and just close to the lower limit (30–80 pM) attained close to the Cape São Vicente by Cotté-Krief et al. (2000). Part of the differences among concentrations can be attributed to three factors: (i) different spatial coverage of the sampling sites varying the distance from the coast, and ii) temporal gap between the surveys with associated variability of the physical, chemical and biological processes, as explained further on, and iii) different analytical methods. The last factor looks quite plausible since with the applied method of acidification, using HCl, only the labile component of the dissolved fraction was measured. Nonetheless, the values were within the same order of magnitude when compared to those from other places under upwelling regimes, such as Finisterre, NW Iberia (Prego et al., 2013), Cape Blanco, NW Africa (Takesue and van Geen, 2002), Californian coast (Biller and Bruland, 2013) and Mejillones Bay, NW Chile (Valdés et al., 2008), as listed in Table 2. At deeper levels the contribution of Mediterranean Water (MW) can be important, as identified by Sánchez et al. (2008), since an upper core flow in equilibrium as shallow as 350 m (Ambar, 1983; Fusco et al., 2008). Few trace metal values are described in the literature for MW crossing the North Atlantic (Boyle et al., 1985; Statham et al., 1985; Sherrell and Boyle, 1988, Van Geen et al., 1988; Béthoux et al., 1990; Yeats, 1998; Elbaz-Poulichet et al., 2001a, 2001b). Those show an increase of metals in the MW mass nearby the Strait of Gibraltar, which may contribute to increase the metals supply during the water uplift.

The concentrations found in the present study are much smaller than those from areas under the influence of rivers contaminated by metals, such as the Tejo and Douro rivers in Portugal (Caetano and Vale, 2003; Leal et al., 1997), Tinto and Odiel (Canovas et al., 2007; Nieto et al., 2007; Elbaz-Poulichet et al., 2001b), and in the Gulf of Cadiz (Van Geen et al., 1991), as shown in Table 2. Dissolved Cd and Pb concentrations are in the range found in other NE Atlantic and shelf waters (Table 2).

In the present study, in transect II, there are no significant resemblances between metals ($p>0.05$). However, significant positive relationships ($p<0.05$, $n=54$) were observed between Zn and nitrate ($r=0.28$), phosphate ($r=0.29$) and silicate ($r=0.32$). These trends are in accordance to the nutrient-like distribution of Zn, as reported by other authors for regions worldwide (Bruland, 1992; Takesue and van Geen, 2002; Franck et al., 2003; Abe, 2004; Biller and Bruland, 2013; Wyatt et al., 2014). In transect IV, a general lack of relationships ($p>0.05$) between metals was found, as pointed out by Cotté-Krief et al. (2000), except between Zn and Cd. Zn was the metal with the highest concentration. In transect IV it showed the lowest concentrations in the upper levels (<50 dbar) of the central stations. It corresponds to those stations where chl *a* and dissolved oxygen increased ($r=-0.27$ and $r=-0.28$ respectively; $p<0.05$). This may suggest that this metal can be removed by an active biological uptake in the surface/near-surface waters. Surface Zn concentrations are known to be very low, as reported for the world's oceans (<50 pM; Bruland and Lohan, 2003; Wyatt et al., 2014). However, it can also indicate a passive scavenging due to adsorption/desorption processes to the phytoplankton cells or other particulate material. Adsorption to organic matter and metal–ligand complexation have been well described in the literature (e.g. González-Dávila, 1995; Brown Jr. and Parks, 2001; Luther III et al., 2001; European Commission, 2002; Bruland and Lohan, 2003; Cobelo-García and Prego, 2004, 2005; Gélabert et al., 2006, 2007; Santos-Echeandía et al., 2012; Baars et al., 2014). The affinity sequence for these metals on metal (oxyhydr)oxide surfaces is particularly high for Pb followed by Zn and then by Cd (Brown Jr. and Parks, 2001). The ligand-bound fraction for Zn could be higher than 98% (Bruland, 1992; Baars and Croot, 2011).

Dissolved Cd, within a much lower order of magnitude (up to 27 pM), decreased to depletion in the upper levels (<75 dbar), like the nutrients (Cravo et al., 2010). This means that this metal may be assimilated and/or adsorbed to phytoplankton, showing a nutrient-type profile, like Zn regardless its biological role (Brown Jr. and Parks, 2001; Morel and Price, 2003). The chemical interaction of phytoplankton by adsorption can also contribute to remove Cd from the water since the ligand-bound fraction could be $>70\%$ (Bruland, 1992). However, in depth, Cd concentrations did not increased and were not particularly correlated with phosphate, as typically found in the ocean (Bruland et al., 1994; de Baar et al., 1994; Yeats, 1998; Biller and Bruland, 2013, among others). Given the low magnitude of concentrations consistently found in levels >200 dbar, this may represent an underestimation of Cd concentrations associated with adsorption processes of Cd to particulate matter, rather than contamination issues linked to the peaks recorded at the intermediate levels. Indeed, the peaks of Cd at levels between 75 and 150 dbar, besides the contribution from the upward of metals from levels around 200 dbar, can derive from the remineralization process below the mixed layer where the biological activity increased, as reflected by the maximum of chl *a* (Cravo et al. (2010, Fig. 6)). Boyle et al. (1981) also reported evidence of Cd regeneration at shallow depths, and like observed for chl *a*, the highest metal concentrations matched the lowest absolute velocities at the frontal boundary between seaward and shoreward flows (Fig. 8). As mentioned in the introduction section, metals can also be accumulated at horizontal interfaces/boundaries where the sinking rates are slow such as in the pycnocline (Pohl et al., 2011). In consequence, the development of phytoplankton during the wind relaxation period may induced an important impact on the metal distributions, and Cd in particular, deviating it from the strong correlations with phosphate (de Baar et al., 1994; Yeats, 1998; Abe, 2004, 2005; Abe et al., 2011; Baars et al., 2014). In the west coast of North America during 1991 and 1993 it was reported that in periods of weaker upwelling, variations in P, Si, and Cd concentrations became uncoupled (van Geen and Husby, 1996). A decoupling of Cd and phosphate cycles after upwelling events has been recently reported due to an intensification of the biological activity after upwelling in the Baja California peninsula, Mexico (Delgadillo-Hinojosa et al. (2015). The

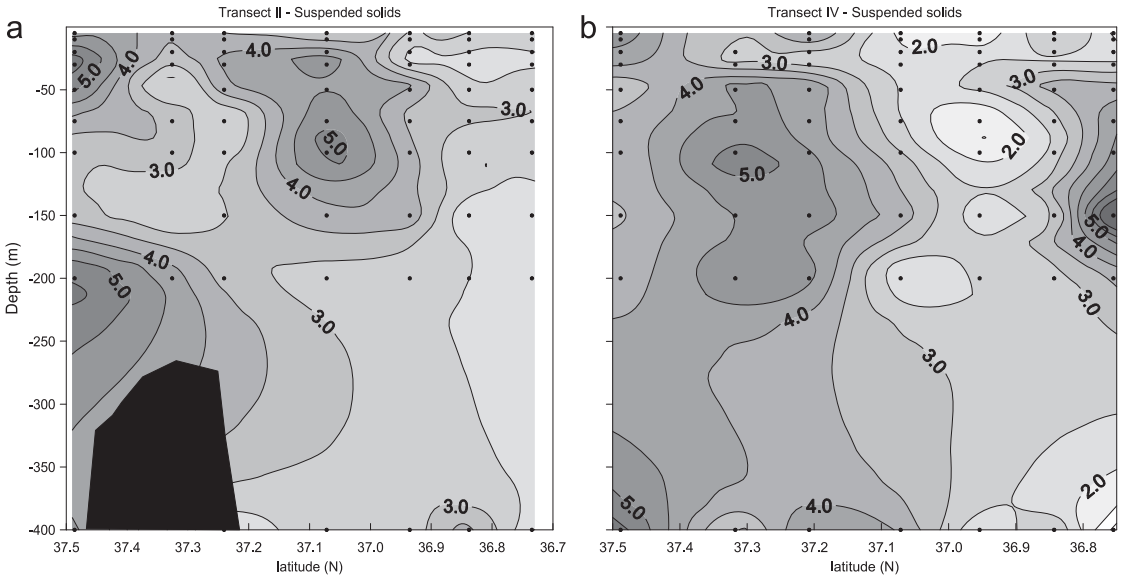

Fig. 10. Vertical fields of suspended solids (mg L^{-1}) in transect II (a) and transect IV (b). Dots represent the sampling points.

authors stated that it is not still well known how Cd concentrations are modified in upwelled waters where there is an increased phytoplankton growth and, in consequence, biological removal of nutrients and trace metals. However, this metal in section II recorded significant negative relationships with temperature ($r=-0.26$, $n=70$; $p<0.05$) and dissolved oxygen ($r=-0.28$; $n=70$; $p<0.05$) supporting the idea of the rise of deeper and colder waters, poorer in oxygen and enriched in Cd.

Lead showed a different behaviour from the other two metals. Apparently, it could suggest that this metal was not associated with upwelling but rather with a northern Pb source, where maximum Pb concentrations (up to 60 pM) were recorded in both transects outside the filament tongue. Pb could be mainly adsorbed onto the phytoplankton cells developed in the filament and scavenged/removed from aqueous solution by high complexation to organic ligands (~98%; Cobelo-García and Prego, 2004). Santos-Echeandía et al. (2012) also point out a diminishing of Pb concentrations during upwelling. The highest concentrations were associated with the maximum of suspended solids (Fig. 10), and in transect IV a positive significant relationship was recorded ($r=0.25$; $n=70$; $p<0.05$). The stations located in the northern areas correspond to a sub-superficial anticyclonic eddy-like feature identified in Sánchez et al. (2008) (see their Fig. 10). These may result from water circulating from the north, advected by the geostrophic equatorward current associated with the upwelling events off the western Iberian coast. The shoreward transport in transect II was higher than that transported seaward (Table 1). However, it remains uncertain what can be the contribution shared by phytoplankton/particles adsorption after upwelling and an external northern source. The sources of this metal to the western margin of Iberian Peninsula are identified as anthropogenic (Prego et al., 2013) and possibly reflect the importance of atmospheric transport into the ocean (Theodosi et al., 2010). Lead could be atmospherically driven (associated to particles) from the northern Sines petrochemical complex, on the western Portuguese coast further north of Cape São Vicente. There, Santos-Echeandía et al. (2012) detected an evident increase of dissolved Pb (20–70 nM). Its atmospheric transport could have been particularly important during the period previous to the cruise, when northerlies were dominant (Fig. 3). There are few available data in literature about atmospheric circulation of Pb in Iberian Peninsula (Jickells, 1995; Kremling and Streu, 2001). Possibly, there is some connection with the metals transport and the high traffic of vessels close to the study area (http://www.marinetraffic.com). Fuel from boats crossing the Cape São Vicente's corridor can still contain some amounts of Pb, despite its decreasing use as an additive in gasoline (Von Storch et al., 2003).

4.2. Filament: causes and consequences for metals

This work provided important field data to better understand the behaviour of the three studied dissolved metals in a filament and did show that there is a clear fingerprint of those metals within an upwelling filament. The filament, comprising 180 t of chl *a* (Cravo et al., 2010), may be considered small in comparison with other filaments observed in areas where upwelling is strong, including those formed in the NW of Iberian Peninsula (Rossi et al., 2013) or in NW Africa (Pastor et al., 2008; Pelegrí et al., 2006, 2005), further south in the Canary Current Upwelling System, or in other Eastern Boundary Upwelling Systems, such as California (Chavez et al., 1991; Jones et al., 1991) and Chile – Bay of Mejillones (Valdés et al., 2008). Even so, and considering that it was sampled in a decaying phase, this filament represented a powerful mechanism of cross-shelf exchange. It exchanged a large amount of water ~1 Sv (Sánchez et al., 2008) along with dissolved and particulate material between the coastal waters and the open ocean.

Unfortunately, data were not found in the literature reporting metal fluxes and transports at cross-sections for other upwelling zones to conduct a reliable comparison of upwelling zones. It can be anticipated that metals transport would be much higher in those areas where filaments can attain hundreds of km. Data reporting metal fluxes across sections from regions other than those under upwelling events are still scarce. Even considering this filament small, it represents an offshore exchange of metals with orders of magnitude higher than those transported to the coast through a small cross-section (0.35 km × 20 m) in the outer channel of the Ferrol Ria (NW Spain), under low river inflow (Zn: 17.5–43.2 kg d^{-1}; Pb: 0.7–3.4 kg d^{-1}; Cobelo-García et al., 2005).

The filament stretching offshore supplies essential metals to phytoplankton and is responsible for the enhancement of the productivity of these more distant waters, typically oligotrophic. Dissolved Pb, on the other hand, having no biological function could represent a spread of a potentially toxic metal in the top 200 dbar of ocean. Nevertheless, as the concentrations were very

low (in the order of pM), close to baseline values, its effect should not be of great concern. It is worthwhile to remark that these metals, either in the filament or in the top 200 dbar, just correspond to the residual concentrations, after consumption by the phytoplankton and/or adsorption processes. So, at the first stages of upwelling, when phytoplankton development is minimal, metal exchanged amounts will be undoubtedly higher. Unfortunately, the contribution of the particulate phase of the three studied metals cannot be estimated because we have no data.

Depending on oceanographic processes and circulation, metal concentrations may change from periods of remineralisation in deeper levels, by internal recycling within the water column and uplift of water during upwelling or downwelling of waters during relaxation. So, to better understand the behaviour and fate of these metals it is crucial to consider joint research embracing physical, chemical and biological processes along the continental shelf of the SW tip off Iberia, encompassing different oceanographic conditions and processes, such as upwelling and periods of wind relaxation, with the consequent development of the coastal countercurrent circulation. Moreover, the particulate fraction of these metals and their relationship with other oceanographic parameters such as pCO_2 (Cullen and Sherrell, 2005), will further improve our knowledge about the biogeochemical cycles and role of these trace metals in the marine environment.

5. Conclusions

An upwelling filament rooted in the Cape São Vicente, the SW limit of the Iberian Peninsula, was surveyed during a relaxation period, just after a long and intense event of coastal upwelling favourable wind. Although of small dimensions relatively to others in areas where upwelling is recurrent, the filament dynamics imposed a remarkable signature in the dissolved metals distribution (Zn, Cd and Pb). It conveyed a large amount of water (0.9 Sv) seaward and important amounts of metals. Regardless some reserve of part of the data, the metals transport estimated for the first time for the SW Iberia after an upwelling event show an export of Zn and Cd inside the filament core comparatively to the surrounding waters. The estimated offshore transports within the filament developed in an area of ~83.5–84.5 km along the top 200 m, range from 295–1560 mmol s^{-1} of zinc, 2–3 mmol s^{-1} of cadmium and 5–16 mmol s^{-1} of lead. As, the filaments formed at Cape São Vicente stand for about 2.5 months these may reach ~10125 kmol for Zn, ~19 kmol Cd and 96 kmol for Pb in a typical year.

The distributions of Zn and Cd, as micronutrients, were affected by the phytoplankton development, notwithstanding of the potential adsorption interaction. On the other hand, concentrations of Pb, as a non-essential metal, must be mainly explained by adsorption processes. Under stronger upwelling conditions the sampled filament can hugely be extended seaward, further transporting higher amounts of metals. Therefore, it will be quite interesting to sample the study area during a period of stronger wind stress, when consumption by phytoplankton or adsorption onto their cells is negligible, to also estimate the upper threshold of the fluxes of material brought to near-surface depths and exported offshore by upwelling.

The concentrations of Zn, Cd and Pb are within the order of magnitude of those found close to this study area and for other upwelling centres, although close to the lower limit, possibly because the quantified fraction in the present study just represents the labile fraction of the dissolved metals.

The quantification of the cross-shelf transports imposed by the filament did show that metals are strong enough to play a key role in the oceanographic behaviour of the zone of transition between the coastal and offshore waters in the region of Cape São Vicente. Considering the periods of intense upwelling events and the extent of their duration, the estimated amounts of exported matter may be hugely increased and micronutrients such as Zn and Cd, along with macronutrients, may contribute to the high productivity of the waters, showing the vital importance of the upwelling filaments to understand the functioning of the regional ecosystem.

Acknowledgements

The authors would like to thank the Project ATOMS, Acoustic Tomography Ocean Monitoring System (PDCTM/P/Mar/15296/99), financed by FCT – Portugal, and to the organisations involved in this work: Instituto Hidrográfico and the University of the Algarve, as well as all the participants in this oceanographic work, with a special thanks to Belisandra Lopes and her help during the trace metal analysis. The authors would also to acknowledge the two anonymous reviewers for the important improvements suggested to the manuscript.

References

Abe, K., 2004. Cadmium distribution in the Western Pacific. In: Shiyomi, M., et al. (Eds.), Global Environmental Change in the Ocean and on Land, pp. 189–203.
Abe, K., 2005. Apparent biological fractionation between Cd and PO_4 in the surface waters of the equatorial Pacific Ocean. Mar. Chem. 96, 347–358.
Abe, K., Fukuoka, K., Shimoda, T., 2011. Characteristics of the ratio of dissolved cadmium to phosphate in subtropical coastal waters of Ishigaki Island, Okinawa, Japan. J. Oceanogr. 67, 241–248.
Abe, K., Matsunaga, K., Igarashi, K., Kudo, I., Fukase, S., 1983. Determination of Cu, Pb, Cd and Zn in seawater by anodic stripping voltammetry. Bull. Fac. Fish. Hokkaido Univ. 34 (4), 350–354.
Alvarez-Salgado, X., Doval, M., Borges, A., Joint, I., Frankignoulle, M., Woodward, E.M., Figueiras, F., 2001. Off-shelf fluxes of labile materials by an upwelling filament in the NW Iberian Upwelling System. Prog. Oceanogr. 51, 321–337.
Ambar, I., 1983. A shallow core of Mediterranean Water off western Portugal. Deep Sea Res. 30, 677–680..
Arístegui, J., Barton, E.D., Álvarez-Salgado, X.A., Santos, A.M.P., Figueiras, F.G., Kifani, S., Hernández-León, S., Mason, E., Machú, E., Demarcq, H., 2009. Sub-regional ecosystem variability in the Canary Current upwelling. Prog. Oceanogr. 83, 33–48.
Baars, O., Abouchami, W., Galer, S., Boye, M., Croot, P., 2014. Dissolved cadmium in the Southern Ocean: distribution, speciation, and relation to phosphate. Limnol. Oceanogr. 59, 385–399.
Baars, O., Croot, P.L., 2011. The speciation of dissolved zinc in the Atlantic sector of the Southern Ocean. Deep Sea Res. Part II: Top. Stud. Oceanogr. 58, 2720–2732.
Béthoux, J.-P., Courau, P., Nicolas, E., Ruiz-Pino, D., 1990. Trace metal pollution in the Mediterranean Sea. Oceanol. Acta 13 (4), 481–488.
Biller, D.V., Bruland, K.W., 2013. Sources and distributions of Mn, Fe, Co, Ni, Cu, Zn, and Cd relative to macronutrients along the central California coast during the spring and summer upwelling season. Mar. Chem. 155, 50–70.
Boyle, E.A., Huested, S.S., Jones, S.P., 1981. On the distribution of copper, nickel, and cadmium in the surface waters of the North Atlantic and North Pacific Ocean. J. Geophys. Res. 86 (C9), 8048–8066.
Boyle, E.A., Chapnick, S.D., Bai, X.X., Spivack, A., 1985. Trace metal enrichments in the Mediterranean Sea. Earth Planet. Sci. Lett. 74, 405–419.
Brown Jr, G.E., Parks, G.A., 2001. Sorption of trace elements on mineral surfaces: modern perspectives from spectroscopic studies, and comments on sorption in the marine environment. Int. Geol. Rev. 43, 963–1073.
Bruland, K.W., 1992. Complexation of cadmium central North Pacific by natural organic ligands in the cadmium complexation. Limnol. Oceanogr. 37, 1008–1017.
Bruland, K.W., Orians, K.J., Cowen, J.P., 1994. Reactive trace metals in the stratified central North Pacific. Geochim. Cosmochim. Acta 58, 3171–3182.
Bruland, K.W., Lohan, M.C., 2003. 6.02 - Controls of Trace Metals in Seawater. In: Holland, H.D., Turekian, K.K.B.T.-T. on G. (Eds.), Treatise on Geochemistry. Pergamon, Oxford, pp. 23–47.
Caetano, M., Vale, C., 2003. Trace-element Al composition of seston and plankton along the Portuguese coast. Acta Oecol. 24, S341–S349.
Canovas, C.R., Olías, M., Nieto, J.M., Sarmiento, aM., Cerón, J.C., 2007. Hydrogeochemical characteristics of the Tinto and Odiel Rivers (SW Spain). Factors controlling metal contents. Sci. Total Environ. 373, 363–382.
Chavez, F.P., Barber, R.T., Kosro, P.M., Huyer, A., Ramp, S.R., Stanton, T.P., Mendiola, B.R., 1991. Distribution of nutrients in the coastal transition zone off Northern California: effects on primary production, phytoplankton biomass and species composition. J. Geophys. Res. 96, 14833–14848.
Chavez, F.P., Messié, M., 2009. A comparison of eastern boundary upwelling ecosystems. Prog. Oceanogr. 83, 80–96.
Cobelo-García, A., Prego, R., 2004. Chemical speciation of dissolved copper, lead and zinc in a ria coastal system: the role of resuspended sediments. Anal. Chim. Acta 524, 109–114.

Cobelo-García, A., Prego, R., DeCastro, M., 2005. Metal distributions and their fluxes at the coastal boundary of a semi-enclosed ria. Mar. Chem. 97, 277–292.
Cotté-Krief, M., Guieu, C., Thomas, A., Martin, J.-M., 2000. Sources of Cd, Cu, Ni and Zn in Portuguese coastal waters. Mar. Chem. 71, 199–214.
Cotté-Krief, M.-H., Thomas, A.J., Martin, J.-M., 2002. Trace metal (Cd, Cu, Ni and Pb) cycling in the upper water column near the shelf edge of the European continental margin (Celtic Sea). Mar. Chem. 79, 1–26.
Cox, A.D., Noble, A.E., Saito, M.A., 2006. Bioavailability of cadmium: Stable isotope uptake and toxicity of Cd to marine phytoplankton in the Costa Rica Upwelling Dome. Geochim. Cosmochim. Acta 70, A114.
Cravo, A., Relvas, P., Cardeira, S., Rita, F., Madureira, M., Sánchez, R., 2010. An upwelling filament off southwest Iberia: effect on the chlorophyll a and nutrient export. Cont. Shelf Res. 30, 1601–1613.
Croot, P.L., Baars, O., Streu, P., 2011. The distribution of dissolved zinc in the Atlantic sector of the Southern Ocean. Deep Sea Res. Part II: Top. Stud. Oceanogr. 58, 2707–2719.
Cullen, J.T., Sherrell, R.M., 2005. Effects of dissolved carbon dioxide, zinc, and manganese on the cadmium to phosphorus ratio in natural phytoplankton assemblages. Limnol. Oceanogr. 50, 1193–1204.
de Baar, H.J.W., Saager, P.M., Nolting, R.F., van der Meer, J., 1994. Cadmium versus phosphate in the world ocean. Mar. Chem. 46, 261–281.
Delgadillo-Hinojosa, F., Camacho-Ibar, V., Huerta-Díaz, M.A., Torres-Delgado, V., Pérez-Brunius, P., Lares, L., Marinone, S.G., Segovia, J.A., Peña-Manjarrez, J.L., García-Mendoza, E., Castro, R., 2015. Seasonal behavior of dissolved cadmium and Cd/PO_4 ratio in Todos Santos Bay: A retention site of upwelled waters in the Baja California peninsula, Mexico. Marine Chemistry 168, 37–48. http://dx.doi.org/10.1016/j.marchem.2014.10.010.
Elbaz-Poulichet, F., Guieu, C., Morley, N.H., 2001a. A reassessment of trace metal budgets in the Western Mediterranean Sea. Mar. Pollut. Bull. 42, 623–627.
Elbaz-Poulichet, F., Morley, N., Beckers, J., Nomerange, P., 2001b. Metal fluxes through the Strait of Gibraltar: the influence of the Tinto and Odiel rivers (SW Spain). Mar. Chem. 73, 193–213.
Ellwood, M., Van den Berg, C., 2000. Zinc speciation in the northeastern Atlantic Ocean. Mar. Chem. 68, 295–306.
European Commission, D.E.E., 2002. Heavy metals in waste, Final Report Project ENV.E.3/ETU/2000/0058.
Fiúza, A.F.G., 1983. Upwelling patterns off Portugal. In: Suess, A.E., Thiede, J. (Eds.), Coastal Upwelling, Part A. Plenum Publishing, New York, pp. 85–98.
Franck, V., Bruland, K., Hutchins, D., Brzezinski, M., 2003. Iron and zinc effects on silicic acid and nitrate uptake kinetics in three high-nutrient, low-chlorophyll (HNLC) regions. Mar. Ecol. Prog. Ser. 252, 15–33.
Fréon, P., Barange, M., Arístegui, J., 2009. Eastern boundary upwelling ecosystems: Integrative and comparative approaches. Prog. Oceanogr. 83, 1–14.
Fusco, G., Artale, V., Cotroneo, Y., Sannino, G., 2008. Thermohaline variability of Mediterranean Water in the Gulf of Cadiz, 1948–1999. Deep Sea Res. Part I: Oceanogr. Res. Pap. 55, 1624–1638.
García-Muñoz, M., Arístegui, J., Montero, M.F., Barton, E.D., 2004. Distribution and transport of organic matter along a filament-eddy system in the Canaries – NW Africa coastal transition zone region. Prog. Oceanogr. 62, 115–129.
Gélabert, A., Pokrovsky, O.S., Reguant, C., Schott, J., Boudou, A., 2006. A surface complexation model for cadmium and lead adsorption onto diatom surface. J. Geochem. Explor. 88, 110–113.
Gélabert, A., Pokrovsky, O.S., Schott, J., Boudou, A., Feurtet-Mazel, A., 2007. Cadmium and lead interaction with diatom surfaces: a combined thermodynamic and kinetic approach. Geochim. Cosmochim. Acta 71, 3698–3716.
González-Dávila, M., 1995. The role of phytoplankton cells on the control of heavy metal concentration in seawater. Mar. Chem. 48, 215–236.
Jickells, T., 1995. Atmospheric inputs of metals and nutrients to the oceans: their magnitude and effects. Mar. Chem. 48, 199–214.
Jones, B.H., Mooers, C.N.K., Rienecker, M.M., Stanton, T., Washburn, L., 1991. Chemical and biological structure and transport of a cool filament associated with a jet-eddy system off Northern California in July 1986 (OPTOMA21). J. Geophys. Res. 96, 22207–22225.
Kremling, K., Streu, P., 2001. The behaviour of dissolved Cd, Co, Zn, and Pb in North Atlantic near-surface waters (301N/601W–601N/21W). Deep Sea Res. I 48, 2541–2567.
Leal, M., Vasconcelos, M., Sousa-pinto, I., 1997. Biomonitoring with benthic macroalgae and direct assay of heavy metals in seawater of the Oporto coast (Northwest Portugal). Mar. Pollut. 34, 1006–1015.
Luther III, G.W., Rozan, T.F., Witter, A., Lewis, B., 2001. Metal-organic complexation in the marine environment. Geochem. Trans. 2, 65.
Moita, T.G., 2001. Estrutura, Variabilidade e Dinâmica do Fitoplâncton na costa de Portugal Continental. Diss. apresentada à Fac. Ciências da Univ. Lisboa para obtenção do grau Doutor em Biol, Lisboa 272 pp.
Morel, F.M., Hudson, R.J.M., Price, N.M., 1991. Limitation of productivity by trace metals in the sea. Limnol. Oceanogr. 36, 1742–1755.
Morel, F.M.M., Price, N.M., 2003. The biogeochemical cycles of trace metals in the oceans. Science 300, 944–947.
Morley, N., Burton, J., Tankere, S., Martin, J.-M., 1997. Distribution and behaviour of some dissolved trace metals in the western Mediterranean Sea. Deep Sea Res. Part II 44, 675–691.
Muller, F.L.L., 1999. Evaluation of the effects of natural dissolved and colloidal organic ligands on the electrochemical lability of Cu, Pb and Cd in the Arran Deep, Scotland. Mar. Chem. 67, 43–60.
Nieto, J.M., Sarmiento, A.M., Olías, M., Canovas, C.R., Riba, I., Kalman, J., Delvalls, T.A., 2007. Acid mine drainage pollution in the Tinto and Odiel rivers (Iberian Pyrite Belt, SW Spain) and bioavailability of the transported metals to the Huelva Estuary. Environ. Int. 33, 445–455.
NRCC, 1992. Open Ocean Seawater Reference Material For Trace Metals. Provisional Certificate. National Research Council Canada, Institute for Environmental Chemistry, Ottawa, Canada.
Pastor, M.V., Pelegrí, J.L., Hernández-Guerra, A., Font, J., Salat, J., Emelianov, M., 2008. Water and nutrient fluxes off Northwest Africa. Cont. Shelf Res. 28, 915–936.
Pelegrí, J.L., Arístegui, J., Cana, L., González-Dávila, M., Hernández-Guerra, a, Hernández-León, S., Marrero-Díaz, a, Montero, M.F., Sangrà, P., Santana-Casiano, M., 2005. Coupling between the open ocean and the coastal upwelling region off northwest Africa: water recirculation and offshore pumping of organic matter. J. Mar. Syst. 54, 3–37.
Pelegrí, J.L., Marrero-Díaz, a, Ratsimandresy, a W., 2006. Nutrient irrigation of the North Atlantic. Prog. Oceanogr. 70, 366–406.
Pohl, C., Croot, P.L., Hennings, U., Daberkow, T., Budeus, G., Loeff, M.R.V.D., 2011. Synoptic transects on the distribution of trace elements (Hg, Pb, Cd, Cu, Ni, Zn, Co, Mn, Fe, and Al) in surface waters of the Northern- and Southern East Atlantic. J. Mar. Syst. 84, 28–41.
Prego, R., Santos-Echeandía, J., Bernárdez, P., Cobelo-García, A., Varela, M., 2013. Trace metals in the NE Atlantic coastal zone of Finisterre (Iberian Peninsula): terrestrial and marine sources and rates of sedimentation. J. Mar. Syst. 126, 69–81.
Relvas, P., Barton, E.D., 2002. Patterns in the Cape São Vicente (Iberian Peninsula) upwelling region. J. Geophys. Res. 107 (C10), 3164.
Relvas, P., Barton, E.D., 2005. A separated jet and coastal counterflow during upwelling relaxation off Cape São Vicente (Iberian Peninsula). Cont. Shelf Res. 25, 29–49.
Relvas, P., Barton, E.D., Dubert, J., Oliveira, P.B., Peliz, Á, da Silva, J.C.B., Santos, aM.P., 2007. Physical oceanography of the western Iberia ecosystem: latest views and challenges. Prog. Oceanogr. 74, 149–173.
Rossi, V., Garçon, V., Tassel, J., Romagnan, J.-B., Stemmann, L., Jourdin, F., Morin, P., Morel, Y., 2013. Cross-shelf variability in the Iberian Peninsula Upwelling System: Impact of a mesoscale filament. Cont. Shelf Res. 59, 97–114.
Saager, P., Baar, H. de, Jong, J. de, 1997. Hydrography and local sources of dissolved trace metals Mn, Ni, Cu, and Cd in the northeast Atlantic Ocean. Mar. Chem. 57, 195–216.
Sánchez, R.F., Relvas, P., Martinho, A., Miller, P., 2008. Physical description of an upwelling filament west of Cape St. Vincent in late October 2004. J. Geophys. Res. 113 (C0704), 1–21.
Santos-Echeandía, J., Prego, R., Cobelo-García, A., 2009. Intra-annual variation and baseline concentrations of dissolved trace metals in the Vigo Ria and adjacent coastal waters (NE Atlantic Coast). Mar. Pol. Bul. 58, 298–303.
Santos-Echeandía, J., Caetano, M., Brito, P., Canario, J., Vale, C., 2012. The relevance of defining trace metal baselines in coastal waters at a regional scale: the case of the Portuguese coast (SW Europe). Mar. Environ. Res. 79, 86–99.
Shaked, Y., Xu, Y., Leblanc, K., Morel, F.M.M., 2006. Zinc availability and alkaline phosphatase activity in Emiliania huxleyi: Implications for Zn-P co-limitation in the ocean. Limnol. Oceanogr. 51, 299–309.
Sherrell, R.M., Boyle, E.A., 1988. Zinc, chromium, vanadium and iron in the Mediterranean Sea. Deep Sea Res. 35 (8), 1319–1334.
Smith, R.L., 1995. The physical processes of coastal ocean upwelling systems, in Upwelling in the Ocean: Modern Processes and Ancient Records. John Wiley, Hoboken, NJ.
Statham, P.J., Burton, J.D., Hydes, D.J., 1985. Cd and Mn in the Alboran Sea and adjacent North Atlantic: geochemical implications for the Mediterranean. Nature 313, 565–567.
Takesue, R., van Geen, A., 2002. Nearshore circulation during upwelling inferred from the distribution of dissolved cadmium off the Oregon coast. Limnol. Oceanogr. 47, 176–185.
Theodosi, C., Markaki, Z., Tselepides, a, Mihalopoulos, N., 2010. The significance of atmospheric inputs of soluble and particulate major and trace metals to the eastern Mediterranean seawater. Mar. Chem. 120, 154–163.
Valdés, J., Román, D., Alvarez, G., Ortlieb, L., Guiñez, M., 2008. Metals content in surface waters of an upwelling system of the northern Humboldt Current (Mejillones Bay, Chile). J. Mar. Syst. 71, 18–30.
Van Geen, A., Boyle, E.A., Moore, W.S., 1991. Trace metal enrichments in waters of the Gulf of Cadiz, Spain. Geochim. Cosmochim. Acta 55, 2173–2191.
Van Geen, A., Rosener, P., Boyle, E., 1988. Entrainment of trace-metal-enriched Atlantic-shelf water in the inflow to the Mediterranean Sea. Nature 331, 423–426.
Van Geen, A., Husby, D.M., 1996. Cadmium in the California Current System: tracer of past and present upwelling. J. Geophys. Res. 101 (C2), 389–3507.
Von Storch, H., Costa-Cabral, M., Hagner, C., Feser, F., Pacyna, J., Pacyna, E., Kolb, S., 2003. Four decades of gasoline lead emissions and control policies in Europe: a retrospective assessment. Sci. Total Environ. 311, 151–176.
Wyatt, N., Milne, A., Woodward, E., Rees, A., Browning, T., Bouman, H., Worsfold, P., Lohan, M., 2014. Biogeochemical cycling of dissolved zinc along the GEOTRACES South Atlantic transect GA10 at 40°S. Glob. Biogeochem. Cycles 28, 44–56.
Yeats, P.A., 1998. An isopycnal analysis of cadmium distributions in the Atlantic Ocean. Mar. Chem. 61, 15–23.